Large-Scale Parameter Estimation in Low-Density Polyethylene Tubular Reactors

ARTICLE *in* INDUSTRIAL & ENGINEERING CHEMISTRY RESEARCH · OCTOBER 2006

Impact Factor: 2.59 · DOI: 10.1021/ie060338n

2 AUTHORS, INCLUDING:

Victor M. Zavala
Argonne National Laboratory
66 PUBLICATIONS **955** CITATIONS

Large-Scale Parameter Estimation in Low-Density Polyethylene Tubular Reactors

Victor M. Zavala and Lorenz T. Biegler*

Department of Chemical Engineering, Carnegie Mellon University, 5000 Forbes Avenue, Pittsburgh, Pennsylvania 15213

We propose a simultaneous approach for the solution of the associated DAE-constrained parameter estimation problem. Parameter estimation is an essential task in the development and on-line update of first-principles models for low-density polyethylene tubular reactors, consisting of nonlinear and stiff differential−algebraic equations (DAE). Our approach discretizes the reactor model equations in space, leading to a large-scale nonlinear program (NLP) that can be solved efficiently with state-of-the-art general-purpose NLP solvers. In doing so, more efficient estimation strategies can be considered, enabling the solution of challenging estimation problems including multiple data and large parameters sets. This approach is efficient in handling advanced regression problems such as the errors-in-variables-measured (EVM) formulation. The methodology is fast, robust, and reliable and can be used both for off-line and on-line purposes. Moreover, substantial improvements on the reactor model predictions have been obtained over previous approaches, making the model amenable for real-time optimization and control tasks.

1. Introduction

The chemical industry faces a challenging and competitive market where high-quality commodity polymers play a central role. These polymers are produced in high-throughput and flexible continuous processes which produce a multitude of polymer grades with tight quality specifications. Stringent performance conditions coupled with high operating costs have motivated the application of advanced real-time optimization and control schemes. These applications require the development of comprehensive first-principles models with accurate predictive capabilities. In all of these developments, a considerable amount of time is spent in discriminating among candidate models and determining the associated parameters.

Low-density polyethylene (LDPE) grades are produced in processes with high-pressure, multizone tubular reactors. Reacting in the gas phase at high temperature (130−300 °C) and pressure (1500−3000 atm), ethylene and a comonomer are copolymerized through a free-radical mechanism[1] in the presence of complex mixtures of peroxide initiators. A typical tubular reactor can be described as a jacketed, multizone device with a predefined sequence of reaction and cooling zones. Different configurations of monomer, comonomer, and initiator mixtures enter in feed and multiple sidestreams and are selected to maximize the reactor productivity and obtain the desired polymer properties. The total reactor length ranges between 0.5 and 2 km, while its internal diameter does not exceed 70−80 mm. A schematic representation of a typical tubular reactor is presented in Figure 1. The final end-use properties of the different LDPE grades are mainly correlated to the polymer density and macromolecular properties. Different additives or chain-transfer agents (CTAs) are added to the axial feed streams to control the polymer melt index. In general, the required polymer properties are enforced through complex recipes that try to keep the reactor under strict operating conditions.

Mathematical modeling of industrial LDPE tubular reactors is a fundamental but difficult task that motivates a huge amount of research effort. A number of comprehensive steady-state tubular reactor models are available in the literature.[2−5] These large-scale models differ in the mechanisms postulated to describe the polymerization kinetics,[6] the prediction approach of the final polymer properties,[7] the prediction methods of the reacting mixture physical properties,[8] assumptions regarding the flow regime, different approaches for taking into account the reactor variability,[9,10] and, finally, the kinetic and transport parameters used for model validation.[4] A common observation in all these studies is the lack of a consistent database of parameters that can be used for model development. Therefore, it is often necessary to re-estimate these parameters using experimental data from the particular laboratory or industrial reactor under study, a complicated and time-consuming task.[5,8]

Well-known parameter estimation theory and methods have been applied only recently to large-scale rigorous process models[11,12] and, in particular, to polymerization reactors models.[13−15] In the particular case of LDPE tubular reactor models, the parameter estimation problem turns out to be so large and complex that it is usually simplified, using heuristics based on the knowledge of the kinetic mechanism.[5,8] As a result, these nonsystematic approaches may yield parameters with large confidence regions, leading to lack of robustness in model predictions over the desired operating range or different reactor configurations.

Although essential for systematic model development, the application of robust and efficient parameter estimation techniques to tubular polymerization reactors models has been limited due to several factors. First, distributed reactor models comprise large sets of complex differential−algebraic equations (DAEs). Accordingly, the associated parameter estimation problem is formulated as a large-scale DAE-constrained optimization problem. The second factor has been the lack of efficient strategies and numerical algorithms able to handle these computationally intensive problems. Finally, estimation problems must be solved using scarce and sometimes noninformative industrial data, giving rise to ill-posed problems with nonunique solutions.

In this work, we present an efficient approach for the solution of parameter estimation problems arising from the development and on-line update of first-principles models for LDPE tubular polymerization reactors. The main idea is to formulate a general multiset parameter estimation problem with a maximum-

* To whom correspondence should be addressed. E-mail: lb01@andrew.cmu.edu. Phone: (412) 268−2232.

10.1021/ie060338n CCC: $33.50
Published on Web 10/07/2006

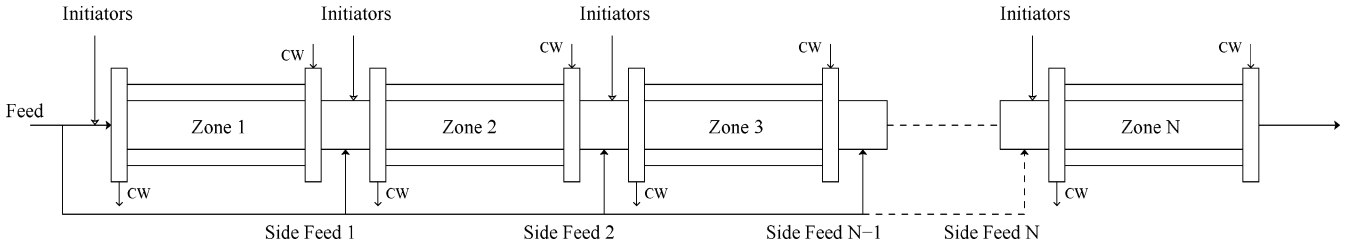

Figure 1. Schematic representation of a typical LDPE tubular reactor.

likelihood objective function subject to a large-scale DAE model. The estimation problem is discretized in space, giving rise to large-scale, structured, and highly nonlinear NLPs. The resulting optimization problems are then solved using the state-of-the-art general-purpose nonlinear program (NLP) interior-point algorithm, IPOPT.[16]

Our study is based on a comprehensive tubular reactor model obtained from extensive literature studies. For the estimation problem, we consider multiple sets of industrial data containing snapshots of the operating conditions of different full-scale industrial reactors configurations that produce several polymer grades. The parameter estimation problem is analyzed from two perspectives. First, we consider estimation of the on-line adjustable parameters. These parameters are estimated to match the reactor temperature profile at different instances of the operation horizon. Next, we consider the estimation of intrinsic kinetic parameters that match the reactor conversion and the macromolecular properties of different grades. An important observation is that, if industrial data are used in the estimation problem, on-line adjustable and kinetic parameters should be estimated simultaneously, giving rise to large, complicated estimation problems. This leads to single estimation problems formulated with multiple data sets, that obtain reliable parameters with tight confidence intervals. Consequently, the model is robust and accurate in predicting the behavior of different reactors over a wide range of conditions. Finally, we show that advanced nonlinear regression methods can be applied efficiently to large-scale rigorous process models with this approach. To illustrate this, we consider both standard least-squares and errors-in-variables-measured (EVM) formulations for the solution of the parameter estimation problem.

The next section presents a comprehensive first-principles LDPE reactor model, followed by formulation of the parameter estimation problems in section 3. The strategy followed for the solution of the DAE-constrained optimization problem is discussed in section 4. We discuss an efficient simultaneous approach based on orthogonal collocation on finite elements. This strategy enables parameter estimation problems to be formulated as large-scale NLPs. Here, the general features of the interior point algorithm used for their solution are analyzed from a parameter estimation point of view. In section 5, we demonstrate the capabilities of the proposed approach for estimation of large sets of on-line adjustable and kinetic parameters for the LDPE reactor model using industrial steady-state data. Finally, the last section presents a summary and set of conclusions, along with discussion of future work to deal with challenging parameter estimation problems.

2. Reactor Mathematical Model

We consider a comprehensive first-principles LDPE tubular reactor model described in references 4 and 17. Due to the complexity of the equations and the lack of space, only the general features of the model are described.

2.1. Model Structure. The first-principles tubular reactor model describes the gas-phase free-radical copolymerization of ethylene with a comonomer (vinyl acetate in this work) in the presence of several different initiators and chain-transfer agents (CTAs) under supercritical conditions. The mechanism postulated to describe the copolymerization kinetics is presented in Table 1. Here, the symbols I_i with $i \in \{1, ..., N_I\}$, $R^\bullet$, M_1, M_2, and S_i with $i \in \{1, ..., N_S\}$ denote the initiators, radicals, monomer, comonomer, and chain-transfer agent (CTA) molecules, respectively. The symbol η_i represents the efficiency of initiator i. The symbols $P_{r,s}$ represent "live" polymer chains ending with a monomer unit—with r monomer units and s comonomer units. Similarly, $Q_{r,s}$ are live polymer chains with r, s degrees of polymerization but ending with a comonomer unit and $M_{r,s}$ are "dead" polymer chains. The respective reaction rates for the monomers, initiators, chain-transfer agents, and live and dead polymer chains can be obtained by combining the reaction rates of the elementary reactions describing their production and consumption. Here, we recognize that a complete description of the polymer chain molecular weight distributions requires an extremely large number of population balances for the polymer chains. To avoid this, the method of single moments[18] is used to describe macromolecular properties of the copolymer. The method of moments is based on the statistical representation of the polymer average molecular weights and the compositional properties in terms of the leading moments of the number chain-length distributions of the live and dead polymer chains. In this model, the univariate number chain-length distributions for $P_{r,s}$, $Q_{r,s}$, and $M_{r,s}$ are considered. Accordingly, the moments of the number chain-length distributions are defined as

$$\lambda_n^i = \sum_{r=1}^{\infty}\sum_{s=1}^{\infty}(r+s)^n R^i(r,s) \quad n \in \{0,1,2\}, \quad i \in \{1,2\} \tag{1}$$

$$\mu_n = \sum_{r=1}^{\infty}\sum_{s=1}^{\infty}(r+s)^n D(r,s) \quad n \in \{0,1,2\} \tag{2}$$

where $R^1(r, s) = [P_{r,s}]$, $R^2(r, s) = [Q_{r,s}]$, and $D(r, s) = [M_{r,s}]$. With this, the number- and weight-average molecular weights, the degrees of long-chain branching (LCB) and short-chain branching (SCB) per 1000 carbon atoms can be expressed in terms of the leading moments of the univariate length-chain distribution.

A typical LDPE tubular reactor consists of a complex configuration of interconnected reaction and cooling zones. Multiple injection points of initiator mixtures, monomer, and CTAs are found along the reactor. The model complexity is often reduced by making some general validated assumptions such as the following: the reacting mixture forms a single supercritical phase, plug flow is observed along the reactor, and net production rates of the radicals and live polymer chains are negligible (quasi-steady-state assumption).[4] Considering this, a

Table 1. Free-Radical Copolymerization Mechanism of Ethylene with a Comonomer

Initiator(s) Decomposition	Incorporation of CTAs
$I_i \xrightarrow{\eta_i k_{di}} 2R \quad i = 1, N_I$	$P_{r,s} + S_i \xrightarrow{k_{spi1}} P_{r+1,s} \quad i = 1, N_S$
	$Q_{r,s} + S_i \xrightarrow{k_{spi2}} Q_{r,s+1} \quad i = 1, N_S$
Chain Initiation	**Termination by Combination**
$R^\bullet + M_1 \xrightarrow{k_{i1}} P_{1,0}$	$P_{r,s} + P_{x,y} \xrightarrow{k_{tc11}} M_{r+x,s+y}$
$R^\bullet + M_2 \xrightarrow{k_{i2}} Q_{0,1}$	$P_{r,s} + Q_{x,y} \xrightarrow{k_{tc12}} M_{r+x,s+y}$
	$Q_{r,s} + Q_{x,y} \xrightarrow{k_{tc22}} M_{r+x,s+y}$
Chain Propagation	**Termination by Disproportionation**
$P_{r,s} + M_1 \xrightarrow{k_{p11}} P_{r+1,s}$	$P_{r,s} + P_{x,y} \xrightarrow{k_{td11}} M_{r,s} + M_{x,y}$
$P_{r,s} + M_2 \xrightarrow{k_{p12}} Q_{r,s+1}$	$P_{r,s} + Q_{x,y} \xrightarrow{k_{td12}} M_{r,s} + M_{x,y}$
$Q_{r,s} + M_1 \xrightarrow{k_{p21}} P_{r+1,s}$	$Q_{r,s} + Q_{x,y} \xrightarrow{k_{td22}} M_{r,s} + M_{x,y}$
$Q_{r,s} + M_2 \xrightarrow{k_{p22}} Q_{r,s+1}$	
Chain Transfer to Monomer	**Backbiting**
$P_{r,s} + M_1 \xrightarrow{k_{fm11}} P_{1,0} + M_{r,s}$	$P_{r,s} \xrightarrow{k_{b1}} P_{r,s}$ or $Q_{r,s}$
$P_{r,s} + M_2 \xrightarrow{k_{fm12}} Q_{0,1} + M_{r,s}$	$P_{r,s} \xrightarrow{k_{b2}} Q_{r,s}$ or $P_{r,s}$
$Q_{r,s} + M_1 \xrightarrow{k_{fm21}} P_{1,0} + M_{r,s}$	
$Q_{r,s} + M_2 \xrightarrow{k_{fm22}} Q_{0,1} + M_{r,s}$	
Chain Transfer to Polymer	**β-Scission of Sec- and Tert-Radicals**
$P_{r,s} + M_{x,y} \xrightarrow{k_{fp11}} P_{x,y} + M_{r,s}$	$P_{r,s} \xrightarrow{k_{\beta 1}} \bar{M}_{r,s} + P_{1,0}$
$P_{r,s} + M_{x,y} \xrightarrow{k_{fp12}} Q_{x,y} + M_{r,s}$	$P_{r,s} \xrightarrow{k_{\beta 2}} \bar{M}_{r,s} + Q_{0,1}$
$Q_{r,s} + M_{x,y} \xrightarrow{k_{fp21}} P_{x,y} + M_{r,s}$	$P_{r,s} \xrightarrow{k_{\beta 1}'} \bar{M}_{r,s} + P_{1,0}$
$Q_{r,s} + M_{x,y} \xrightarrow{k_{fp22}} Q_{x,y} + M_{r,s}$	$P_{r,s} \xrightarrow{k_{\beta 2}'} \bar{M}_{r,s} + Q_{0,1}$
Chain Transfer to CTAs	
$P_{r,s} + S_i \xrightarrow{k_{si1}} P_{1,0} + M_{r,s} \quad i = 1, N_S$	
$Q_{r,s} + S_i \xrightarrow{k_{si2}} Q_{0,1} + M_{r,s} \quad i = 1, N_S$	

set of steady-state differential molar balances describing the evolution of the reacting mixture along each zone can be derived. The molar flow rate F_j for every component j in the mixture can be expressed in terms of the fluid velocity, v, and its molar concentration C_j,

$$F_j = vAC_j \tag{3}$$

where A is the reactor cross-sectional area at the given reactor axial position. According to this, the design equations for each reactor zone are given by the following set of differential and algebraic equations:

Initiator(s)

$$\frac{dF_{Ii}}{dz} = -\frac{1}{v} k_{di} F_{Ii} \quad i \in \{1, ..., N_I\} \tag{4}$$

Monomer and Comonomer

$$\frac{dF_{mi}}{dz} = -\frac{F_{mi}}{v}\left(k_{Ii} C_R + \sum_{j=1}^{2} k_{pji} \lambda_0^j + \sum_{j=1}^{2} k_{fmji} \lambda_0^j\right) \quad i \in \{1, 2\} \tag{5}$$

Chain-Transfer Agent(s)

$$\frac{dF_{Si}}{dz} = -\frac{F_{Si}}{v}\left(\sum_{j=1}^{2} k_{sij}\lambda_0^j + \sum_{j=1}^{2} k_{spij}\lambda_0^j\right) \quad i \in \{1, ..., N_S\} \quad (6)$$

Primary Radicals

$$F_R = \frac{A}{(k_{I1}F_{m1}+k_{I2}F_{m2})}\left(v\sum_{i=1}^{N_I} 2\eta_i k_{di}F_{Ii}\right) \quad (7)$$

Energy Balances

$$F_T C_p \frac{dT}{dz} = (-\Delta H_{r1})(k_{p11}\lambda_0^1 + k_{p21}\lambda_0^2)F_{m1}/v + (-\Delta H_{r2})(k_{p12}\lambda_0^1 + k_{p22}\lambda_0^2)F_{m2}/v + F_c C_{pc}\frac{dT_c}{dz} \quad (8)$$

$$F_c C_{pc}\frac{dT_c}{dz} = \pi D_i(\mathrm{HTC})(T_c - T) \quad (9)$$

Momentum Equation

$$\frac{dP}{dz} = -2f_r\frac{\rho_m v^2}{D_i}\frac{1}{101325} \quad (10)$$

Long-Chain Branching (LCB) and Short-Chain Branching (SCB)

$$\frac{1}{A}\frac{dF_{LCB}}{dz} = \sum_{i=1}^{2}(k_{fpi1} + k_{fpi2})\lambda_0^i\mu_1 \quad (11)$$

$$\frac{v}{A}\frac{dF_{SCB}}{dz} = v\left(\sum_{i=1}^{2} k_{bi}\lambda_0^i\right) + \frac{1}{A}\sum_{j=1}^{N_S}(k_{spj1}\lambda_0^1 + k_{spj2}\lambda_0^2)F_{Sj} \quad (12)$$

Dead Polymer Chains Moments

$$\frac{1}{A}\frac{dF_{\mu 0}}{dz} = \sum_{i=1}^{2}\Delta_i\lambda_0^i + \frac{1}{2}\sum_{i=1}^{2}\sum_{j=1}^{2}k_{tcij}\lambda_0^i\lambda_0^j - \mu_1\sum_{i=1}^{2}\sum_{j=1}^{2}k_{fpij}\lambda_0^i \quad (13)$$

$$\frac{1}{A}\frac{dF_{\mu 1}}{dz} = \sum_{i=1}^{2} C_{mi}\left(\sum_{j=1}^{2} k_{pji}\lambda_0^j\right) \quad (14)$$

$$\frac{1}{A}\frac{dF_{\mu 2}}{dz} = 2\sum_{i=1}^{2}\sum_{j=1}^{2}k_{pji}\lambda_1^j C_{mi} + \sum_{i=1}^{2}\sum_{j=1}^{2}k_{tcij}\lambda_1^i\lambda_1^j \quad (15)$$

where

$$\Delta_i = \sum_{j=1}^{2} k_{fmij}C_{mj} + \sum_{j=1}^{N_S} k_{sji}C_{sj} + \sum_{j=1}^{2} k_{tdij}\lambda_0^j + \sum_{j=1}^{2} k_{fpij}\mu_1 + k_{\beta i} + k'_{\beta i} \quad i \in \{1, 2\} \quad (16)$$

Live Polymer Chain Moments

$$F_{\lambda_0^1} = \sqrt{\frac{G^*}{E}} \quad (17)$$

$$F_{\lambda_0^2} = aF_{\lambda_0^1} \quad (18)$$

$$F_{\lambda_1^1} = uA\frac{B_1\Gamma_1^* - A_2\Gamma_1^*}{A_1 - B_1B_2} \quad (19)$$

$$F_{\lambda_1^2} = uA\frac{-\Gamma_2^* - B_2\lambda_1^1}{A_2} \quad (20)$$

where

$$a = \frac{(k_{fm12} + k_{p12})F_{m2} + k_{fp12}F_{\mu 1}}{(k_{fm21} + k_{p21})F_{m1} + k_{fp21}F_{\mu 1}} \quad (21)$$

$$E = (k_{td11} + k_{tc11}) + 2a(k_{td12} + k_{tc12}) + a^2(k_{td22} + k_{tc22}) \quad (22)$$

$$G^* = (k_{I1}F_{m1} + k_{I2}F_{m2})F_R \quad (23)$$

$$A_1 = -(k_{p12}C_{m2} + \Delta_1 + \sum_{j=1}^{2} k_{tc1j}\lambda_0^j) \quad (24)$$

$$A_2 = -(k_{p21}C_{m1} + \Delta_2 + \sum_{j=1}^{2} k_{tc2j}\lambda_0^j) \quad (25)$$

$$B_1 = k_{p21}C_{m1} \quad (26)$$

$$B_2 = k_{p12}C_{m2} \quad (27)$$

$$\Gamma_i^* = (k_{Ii}C_R + \sum_{j=1}^{2} k_{fmji}\lambda_0^j + \sum_{j=1}^{2} k_{pji}\lambda_0^j)C_{mi} + \lambda_0^i\left(\sum_{j=1}^{N_S} k_{sji}C_{sj} + \sum_{j=1}^{N_S} k_{spji}C_{sj}\right) + \mu_2\left(\sum_{j=1}^{2} k_{fpji}\lambda_0^j\right) + (k_{\beta i} + k_{\beta i}')\lambda_0^i \quad (28)$$

Here, the fluid velocity v is calculated from the total molar flow rate and the mixture density at the corresponding operating conditions. It is important to notice that the primary radicals and the live polymer moment flow rates are algebraic variables. From the schematic representation of the reactor, we can see that the initial conditions of the differential equations are determined from material balances at the axial feed points.

Macromolecular properties of the polymer can be obtained in terms of the leading moments of the univariate chain-length distributions. Accordingly, the polymer number- and weight-average molecular weights and polydispersity are given by

$$MW_n = MW_0\frac{F_{\mu 1}}{F_{\mu 0}} \quad (29)$$

$$MW_w = MW_0\frac{F_{\mu 2}}{F_{\mu 1}} \quad (30)$$

$$PDI = \frac{MW_w}{MW_n}$$

where MW_0 is the average molecular weight of a building unit in the polymer chain. The number of short- and long-chain branches per 1000 atoms can be obtained from

$$LCB = 500\frac{F_{LCB}}{F_{\mu 1}} \quad (31)$$

$$\mathrm{SCB} = 500\,\frac{F_{\mathrm{SCB}}}{F_{\mu 1}} \tag{32}$$

and finally, the polymer density ρ_{pol} is correlated to the number of short-chain branches per 1000 carbon atoms,

$$\rho_{\mathrm{pol}} = c_0 + c_1\mathrm{SCB} \tag{33}$$

where c_0 and c_1 are correlation parameters.

The accuracy of the tubular reactor model depends strongly on the appropriate prediction of the reacting mixture properties. Most of the model complexity comes from the large number of algebraic equations required for the calculation of the mixture physical, thermodynamic, and transport properties. The properties that have more influence on the model accuracy are the mixture density, heat capacity, and viscosity. The gas-phase density and heat capacity are obtained by means of a generalized correlation, based on a three-parameter corresponding states model,[19] while the rest of the properties are obtained from complex semiempirical correlations. All the correlations used have been validated experimentally and are reported elsewhere.[4]

In summary, a typical tubular reactor model with around 10−13 zones can contain up to 300−400 ordinary differential equations (ODEs) and 1000−2000 algebraic equations. This is a highly nonlinear, stiff large-scale DAE model which is computationally expensive and requires a robust and efficient solution algorithm.

2.2 Model Parameters. One of the most difficult problems in simulating the operation of high-pressure LDPE reactors is the selection of appropriate values for the kinetic parameters. Under general assumptions, model equations do not depend on the absolute values of the kinetic rate constants but on predefined ratios of these parameters.[20] However, among literature studies, the actual ratios and values of the kinetic constants differ sometimes by orders of magnitude. Furthermore, it is well-known that kinetic and transport phenomena mask each other in polymerization reactors.[21] As a result, it is still difficult to find a reliable and consistent set of parameters for the model at hand and, obviously, the best approach to tackle this problem is to estimate the parameters using the detailed reactor model to match industrial reactor data.

LDPE tubular reactors are also subject to persistent variability over the operating horizon. This requires the selection and on-line estimation of adjustable parameters to account for this variability. One of the most fundamental and complex problems associated with the operation of LDPE tubular reactors is the severe and random fouling of the inner reactor wall due to a continuous polymer buildup. This phenomenon is difficult to predict by means of simple mechanistic models.[22] There are two simple engineering ways to handle this problem. The first one involves the development of semiempirical correlations in terms of the Reynolds number, polymer composition, and some other variables aiming at the prediction of the polymer fouling resistance evolution along the reactor.[23] While this approach has given relatively good results, the correlation is only useful for the problem at hand and does not capture the evolution of the polymer buildup over time, which is the true motivation for the on-line adjustment of the reactor model.[8,9] The second approach includes two alternatives. If a detailed heat transfer model is available, the fouling resistance can be estimated for each zone to match the plant reactor temperature profile.[17] Here, it is assumed that the fouling resistance is constant along each zone. In the absence of a heat transfer model, the heat transfer coefficients (HTCs) can be defined directly as adjustable parameters in each zone.

As illustrated in Figure 1, a number of sidestream feeds of initiator mixtures or cocktails are distributed along the reactor. At each feed point, a typical mixture can include up to four different initiators with different chemical properties. These initiators decompose to generate the radicals that start the polymerization. The initiator decomposition reactions include sets of complex reaction subnetworks involving the formation of highly active intermediate species that can react among each other or with impurities in the reacting mixture before generating the desired radicals. Thus, there is an efficiency factor η_i associated with the decomposition of each initiator. These initiator efficiencies are strongly dependent on a large number of factors such as the reacting mixture temperature and pressure, the degree of mixing at the feed points, and the presence of other species such as impurities or CTAs. Moreover, the efficiency of an individual initiator might vary with its concentration in the reacting mixture.[24,25] In LDPE tubular reactors, wide variations of the reacting mixture temperature, pressure, composition, and physical properties are observed. As a consequence, wide variations of the efficiencies are expected as well along the reactor and over time due to the accumulation of impurities. To predict the initiator efficiencies observed in LDPE reactors, these can be modeled as parallel reactions with given decomposition constants that generate undesired species.[2,10] Alternatively, the initiator efficiency for each reaction can be estimated for each reaction zone in order to match the plant reactor temperature profile. Previous studies have shown satisfactory results using this approach. To simplify the parameter estimation task, it is usually assumed that there is a common efficiency for all the initiators in the mixture.[17] While this assumption provides sufficiently accurate model predictions, it is expected that the estimation of the individual initiator efficiencies will result in a better match of the plant reactor temperature profile. This is the approach followed in this work.

3. Parameter Estimation Problem Formulation

In each zone, the reactor model is composed of individual sets of differential and algebraic equations describing the evolution of the reacting mixture and cooling agent temperatures. These individual sets are connected through balances at the feed points, thus leading to a large, highly nonlinear system of DAEs for the reactor system. The overall model is defined by the following:

$$\mathbf{F}_j\left[\frac{\mathrm{d}y_j(z)}{\mathrm{d}z}, y_j(z), w_j(z), z, p_j, \Pi\right] = 0$$

$$\mathbf{G}_j[y_j(z), w_j(z), z, p_j, \Pi] = 0$$

$$y_j(0) = \phi(y_{j-1}(z_{\mathrm{L}_{j-1}}), F_{\mathrm{f}_j})$$

$$j \in \{1, ..., \mathrm{NZ}\} \tag{34}$$

Here, $\mathbf{F}_j(.)$ and $\mathbf{G}_j(.)$ are vectors of differential and algebraic equations, respectively, in zone $j \in \{1, ..., \mathrm{NZ}\}$ where NZ is the number of zones in the reactor and z denotes the axial position along each zone. The vector $\mathbf{F}_j(.)$ includes all the differential material and energy balances in the model. The vector $\mathbf{G}_j(.)$ includes all the kinetic Arrhenius-type equations, the expressions defining the reacting mixture properties, and the balances at the feed points along each zone j. The symbols y_j and w_j represent vectors of differential and algebraic variables, respectively, for zone j. Here, the initial conditions $y_j(0)$ for zone j are obtained from material and energy balances $\phi(.)$ at the feed

points relating the outlet stream of zone $j-1$ given by $y_{j-1}(z_{L_{j-1}})$ (where z_{Lj} is the total length of zone j) and the side feeds F_{f_j}. An important observation here is that the reactor model can be solved either sequentially, by solving the DAEs for one zone at a time, or simultaneously, by including the coupled DAE sets and the feed point balances of all the zones in a single large problem. From the reactor model, we can distinguish between two different sets of parameters, the first set p_j are parameters that correspond *exclusively* to the particular zone j; this includes, for example, the heat transfer coefficient and the multiple initiator efficiencies of zone j. The second set of parameters Π corresponds to those parameters that are defined for the *entire* reactor. These parameters include the kinetic rate constants. Clearly, to capture the interaction of parameters p_j and Π, a simultaneous solution of the overall reactor model is needed.

3.1. Standard Least-Squares Formulation. Once the overall reactor model is defined, a proper objective function needs to be selected for the parameter estimation problem. In a standard estimation problem, the model parameters p_j and Π are selected to minimize the deviation between the predicted and the measured values of a set of output variables. Here, a subset of the output variables is defined from differential variables at particular positions of a given zone j, for example, the reacting mixture temperatures and the inlet and outlet cooling water temperatures. A second subset of output variables corresponds to the overall reactor conversion, polymer density, number- and weight-average molecular weights, and LCB at the reactor outlet. Finally, the parameter estimation problem must include multiple data sets describing the different operating conditions or reactor configurations and corresponding values of their output variables. This implies that the large-scale reactor model (35) needs to be defined for every data set $k \in \{1, ..., NS\}$ where NS is the number of data sets. With this, the general parameter estimation problem can be stated as

$$\min_{\Pi, p_{k,j}} \sum_{k=1}^{NS} \sum_{j=1}^{NZ} \sum_{i=1}^{NM(j)} (y_{k,j}(z_i) - y^{M}_{k,j,i})^{T} \mathbf{V}_y^{-1} (y_{k,j}(z_i) - y^{M}_{k,j,i}) + \sum_{k=1}^{NS} (w_{k,NZ} - w^{M}_{k,NZ})^{T} \mathbf{V}_w^{-1} (w_{k,NZ} - w^{M}_{k,NZ})$$

s.t.

$$\mathbf{F}_{k,j}\left[\frac{dy_{k,j}(z)}{dz}, y_{k,j}(z), w_{k,j}(z), z, p_{k,j}, \Pi, u_{k,j}\right] = 0$$

$$\mathbf{G}_{k,j}[y_{k,j}(z), w_{k,j}(z), z, p_{k,j}, \Pi] = 0$$

$$y_{k,j}(0) = \phi(y_{k,j-1}(z_{L_{k,j-1}}), F_{f_{k,j}})$$

$$j \in \{1, ..., NZ\}, \quad k \in \{1, ..., NS\} \tag{35}$$

where NM(j) is the number of measurement positions along zone j, z_i are specific measurement locations along a particular zone j, the symbol M denotes the actual plant measurements, and $\mathbf{V}_y^{-1}$ and $\mathbf{V}_w^{-1}$ denote positive-definite weighting matrices for the output variables, with $\mathbf{V}_y$ and $\mathbf{V}_w$ representing approximations of the corresponding covariance matrices.

The complexity of these problems relies on the fact that the overall reactor model needs to be solved for every data set included in the problem. Therefore, the number of DAE constraints increases linearly with the number of data sets. For example, a problem with a single data set contains around 300−400 ODEs and 1000−2000 algebraic equations while a problem with 5 data sets will contain 1500−2000 ODEs and 5000−10 000 algebraic equations.

3.2. Errors-in-Variables-Measured (EVM) Formulation. The standard least-squares formulation considers errors that are only present in the output variables. This approach is well-known to give biased parameters.[26,27] In the errors-in-variables-measured (EVM) estimation formulation, on the other hand, both errors in the input and output variables are taken into account.[28] For complex systems with multiple inputs such as LDPE tubular reactors, this approach is particularly useful in finding more reliable kinetic parameters. A major difficulty in solving this problem is that, since the error is accounted for in all the variables, the optimization is performed on both the parameters and the inputs, thus leading to problems with many degrees of freedom. The general EVM formulation resembles that of the standard least-squares (35) but, in this case, the inputs for every zone j in every data set k are decision variables. Upon addition of terms in the objective function that account for allowed adjustments from measured input variables, the parameter estimation problem becomes

$$\min_{\Pi, p_{k,j} u_{k,j}} \sum_{k=1}^{NS} \sum_{j=1}^{NZ} \sum_{i=1}^{NM(j)} (y_{k,j}(z_i) - y^{M}_{k,j,i})^{T} \mathbf{V}_y^{-1} (y_{k,j}(z_i) - y^{M}_{k,j,i}) + \sum_{k=1}^{NS} (w_{k,NZ} - w^{M}_{k,NZ})^{T} \mathbf{V}_w^{-1} (w_{k,NZ} - w^{M}_{k,NZ}) + \sum_{k=1}^{NS} \sum_{j=1}^{NZ} (u_{k,j} - u^{M}_{k,j})^{T} \mathbf{V}_u^{-1} (u_{k,j} - u^{M}_{k,j})$$

s.t.

$$\mathbf{F}_{k,j}\left[\frac{dy_{k,j}(z)}{dz}, y_{k,j}(z), w_{k,j}(z), z, p_{k,j}, \Pi, u_{k,j}\right] = 0$$

$$\mathbf{G}_{k,j}[y_{k,j}(z), w_{k,j}(z), z, p_{k,j}, \Pi] = 0$$

$$y_{k,j}(0) = \phi(y_{k,j-1}(z_{L_{k,j-1}}), u_{k,j})$$

$$j \in \{1,..NZ\}, k \in \{1, ..., NS\} \tag{36}$$

where $\mathbf{V}_u^{-1}$ is a positive-definite weighting matrix for the input variables and $u_{k,j}$ and $u^{M}_{k,j}$ are the calculated and measured values of the input variables. Notice that, in this formulation, a multitude of side feeds (monomer, comonomer, CTAs) to the tubular reactor $F_{f_{k,j}}$ correspond to the input variables and appear explicitly in the connectivity equations. Some other inputs included in the formulation are the reactor inlet pressure, feed, and side stream temperatures and the cooling water flow rates and temperatures. This estimation approach corrects for measurement errors on all these variables and is specially useful in obtaining more reliable kinetic parameters. However, as expected, the degrees of freedom in the estimation problems increase linearly with the number of data sets. Consequently, solutions of EVM problems are often considered to be computationally expensive.

4. Solution Strategy

Two main approaches are used for the solution of the DAE-constrained optimization problems described in the previous section. First, the sequential or feasible-path approach separates the model solution and optimization tasks. Instead, the optimizer

updates the parameters and passes them to the DAE solver, which integrates the model equations.[29] Derivative information required by the optimizer can be obtained through the integration of sensitivity or adjoint equations or by perturbation.[30−33] Since this approach requires the repeated solution of the DAE system, it can be computationally demanding for large-scale models. Furthermore, the optimization task becomes much more expensive for problems with multiple data sets, large parameter sets or EVM formulations, thus requiring the decomposition of the original problem through the solution of sequences of smaller subproblems.[11] Nevertheless, because of its relative simplicity in developing solution frameworks from standard optimization and integration algorithms, this approach has been popular for the solution of parameter estimation problems involving DAE models. Also, feasible path approaches are reliable even for stiff nonlinear DAEs, do not require special initialization strategies, and can handle the complexity of the DAEs efficiently.

In the simultaneous or infeasible-path approach, the DAE model solution and optimization tasks are completely coupled by performing a full discretization of the DAE model. With this, the DAE-constrained optimization problem is converted into a large-scale, structured NLP problem. The most important advantage of this approach is that it avoids repeated solution of the large-scale model; it is solved only once, at the solution of the optimization problem. The recent potential of this approach has been directly related to the availability of computational resources, optimization strategies, and high-performance scientific computing routines able to handle large-scale optimization problems.[34] Nowadays, state-of-the-art, general-purpose nonlinear programming algorithms based on sequential quadratic programming (SQP) and interior point (IP) methods can efficiently handle NLP problems with over a million of variables, thus enabling the solution of very challenging optimization problems.[35−37] In particular, these amenities are provided in IPOPT, a general-purpose nonlinear programming interior point algorithm.[16] Furthermore, application of simultaneous approaches has become simple and efficient, due to the availability of powerful modeling environments such as AMPL and GAMS.[38,39] Moreover, these platforms provide exact first and second derivative information, thus enhancing the convergence properties of the optimization algorithm. Simultaneous approaches have been demonstrated for the solution of general DAE- and PDAE-constrained optimization problems in many areas of science and engineering, have been shown to be robust and efficient,[35,40,41] and are superior to sequential approaches on problems with many degrees of freedom.[42] On the other hand, this approach requires careful initializations and might suffer from numerical difficulties associated with the discretization of highly nonlinear and stiff DAEs.

4.1. Model Discretization. In this work, a simultaneous approach based on orthogonal collocation on finite elements was used for the solution of the parameter estimation problem. This discretization scheme approximates the differential and algebraic variable profiles by using a family of interpolation polynomials. The entire axial length along each reactor zone is divided into finite elements ($z_0 < z_1 < ... < z_{NFE} = z_L$). Here, we use a monomial basis representation for the differential profiles[43] that is particularly attractive since it leads to better condition numbers of the Jacobian matrix

$$y(z) = y_{i-1} + h_i \sum_{q=1}^{NC} \Omega_q \left(\frac{z - z_{i-1}}{h_i} \right) \frac{dy}{dz_{i,q}} \tag{37}$$

where y_{i-1} is the value differential variable evaluated at the beginning of element i, $h_i = z_i - z_{i-1}$ is the length of the element i, $dy/dz_{i,q}$ is the value of the first derivative in element i at collocation point q, and Ω_q is an interpolation polynomial of order NC that satisfies

$$\Omega_q(0) = 0 \quad \text{for } q \in \{1, ..., NC\}$$

$$\Omega_q(\rho_r) = \delta_{q,r} \quad \text{for } q \in \{1, ..., NC\}$$

where ρ_r is the location of the rth collocation point within each element and $\delta_{q,r}$ is the Kronecker delta. Continuity of the differential profiles across elements is directly enforced by

$$y_i = y_{i-1} + h_i \sum_{q=1}^{NC} \Omega_q(1) \frac{dy}{dz_{i,q}} \tag{38}$$

Here, Radau collocation points are used because they stabilize the system more efficiently in the presence of high-index DAEs. The algebraic profiles are approximated using a similar monomial basis representation

$$w(z) = \sum_{q=1}^{NC} \psi_q \left(\frac{z - z_{i-1}}{h_i} \right) w_{i,q} \tag{39}$$

where $w_{i,q}$ represents the values of the algebraic variables. ψ_q is a Lagrange polynomial of order NC satisfying

$$\psi_q(\rho_r) = \delta_{q,r} \quad \text{for } q, r \in \{1, ..., NC\}$$

Note that the number and length of the finite elements can be adjusted according to the precision required in the approximation. This flexibility allows the size of the discretized reactor model to be reduced. Also, the objective function in problem (35)−(36) may include measurements located at positions that may not coincide with the mesh. Rather, the calculated values for the measurements can be interpolated along each zone to the closest point in the mesh without losing much accuracy in the results.

Upon substitution of the algebraic expressions (37)−(39) in (35)−(36), these parameter estimation problems can be expressed as large-scale, structured NLP problems of the form

$$\begin{aligned} &\min f(x) \\ &\text{s.t.} \quad c(x) = 0 \\ &x_L \le x \le x_U \end{aligned} \tag{40}$$

where $x \in \mathcal{R}^{nx}$ represents all the variables obtained from the discretization of the DAE.

4.2. NLP Algorithm. The NLP problem (40) is solved using IPOPT, which handles variable bounds by adding a barrier function to the objective made up of logarithmic terms

$$\begin{aligned} &\min \varphi_\mu(x) = f(x) - \mu\left[\sum_{i=1}^{nx} \ln(x^{(i)} - x_L^{(i)}) + \sum_{i=1}^{nx} \ln(x_U^{(i)} - x^{(i)})\right] \\ &\text{s.t.} \quad c(x) = 0 \end{aligned} \tag{41}$$

where μ is a barrier parameter satisfying $\mu > 0$. Under mild regularity conditions, solutions of (40) converge to the solution of (40) as $\mu \to 0$.[44] At a particular value of μ, the primal-dual optimality conditions of (41) resemble those of the original NLP problem and are defined by

$$\nabla_x f(x) + \nabla_x c(x)\lambda - \nu_L + \nu_U = 0$$
$$c(x) = 0$$
$$(X - X_L)V_L e - \mu e = 0$$
$$(X_U - X)V_U e - \mu e = 0 \quad (42)$$

where X, X_L, X_U, V_L, $V_U \in \mathscr{R}^{nx \times nx}$ are diagonal matrixes whose diagonal entries are the components of x, x_L, x_U,ν_L, and ν_U, respectively; $e = [1, 1, ..., 1]^T \in \mathscr{R}^{nx}$, λ is the vector of Lagrange multipliers for the equality constraints; and ν_L, $\nu_U \in \mathscr{R}^{nx}$ is an estimate of the multipliers for the bound constraints of the original NLP problem. The optimality conditions can be solved efficiently by applying Newton's method, which requires the solution of a large and sparse linear system at each iteration given by

$$\begin{bmatrix} \nabla_{x,x} L_k + \Sigma_k & \nabla_x c(x_k) \\ \nabla_x{}^T c(x_k) & 0 \end{bmatrix} \begin{pmatrix} \Delta x_k \\ \Delta \lambda_k \end{pmatrix} = - \begin{pmatrix} \nabla_x \varphi(x_k) + \nabla c(x_k)\lambda_k \\ c(x_k) \end{pmatrix} \quad (43)$$

where L_k is the Lagrangian function of the original NLP problem (40) evaluated at iteration k, Σ_k is defined by

$$\Sigma_k = (X_k - X_L)^{-1} V_L^k + (X_U - X_k)^{-1} V_U^k$$
$$\nabla_x \varphi(x,k) = \nabla_x f(x_k) + (X_k - X_L)^{-1}\mu e + (X_U - X_k)^{-1}\mu e \quad (44)$$

and the bound multipliers are updated at each iteration from

$$\Delta \nu_L^k = (X_k - X_L)^{-1}(\mu e - V_L^k \Delta x_k) - \nu_L^k \quad (45)$$

$$\Delta \nu_U^k = (X_U - X_k)^{-1}(\mu e + V_U^k \Delta x_k) - \nu_U^k \quad (46)$$

The solution of linear system (43) is the core step of the optimization algorithm and requires most of the computational time. This sparse linear system can be solved efficiently using robust factorization algorithms, such as the one implemented in Harwell routine MA27.[45] It is worth emphasizing that exploiting the sparsity of the linear system is fundamental in large-scale optimization. Moreover, ill-conditioning is encountered in this particular application due to poor model scaling and high parametric sensitivity typical of polymerization reactors. This is overcome through a user-specified scaling of the model equations or automatically through equilibration algorithms for the linear system, such as the one implemented in Harwell subroutine MC19.

Global convergence of the algorithm is promoted using a novel filter line search strategy. Line search methods require the Hessian matrix $H_k = \nabla_{x,x} L_k + \Sigma_k$ to have strictly positive curvature in the null space of the linearized constraint gradients. Moreover, under the assumption that $\nabla_x c(x_k)$ has full rank, the projection of H_k onto the null space of $\nabla_x{}^T c(x_k)$ is positive definite if and only if the iteration matrix in (43) has n positive and m negative eigenvalues. However, due to severe nonlinearity of the problem or noninformative data, respectively, the linear independence and positive curvature conditions may not hold at intermediate iterations. To correct for this, IPOPT adds diagonal correction terms to the (so-called KKT) matrix in (43), leading to

$$\begin{bmatrix} \nabla_{x,x} L_k + \Sigma_k + \delta_1 I & \nabla_x c(x_k) \\ \nabla_x{}^T c(x_k) & -\delta_2 I \end{bmatrix} \quad (47)$$

for some δ_1, $\delta_2 > 0$. To detect whether a modification of the Hessian is necessary, the inertia of this iteration matrix (i.e., the number of positive, negative, and zero eigenvalues) can be calculated from MA27 and monitored by the algorithm.[16] An important observation here is that, if the diagonal terms δ_1 and δ_2 are zero at the solution, then the system has the correct inertia, n positive and m negative eigenvalues, and the second order sufficient conditions hold. From a statistical perspective, this gives the important result that the parameters have been uniquely determined and the data are sufficiently informative.

Finally, the algorithm implemented in IPOPT is robust and efficient in solving problems with many degrees of freedom if exact second derivative information is provided.[47] This is done automatically through specialized automatic differentiation routines implemented in AMPL. This feature is particularly important for solving estimation problems with many parameters, such as those arising from EVM formulations.

5. Industrial Case Studies and Results

We now consider the parameter estimation for the LDPE reactor model. Several industrial data sets have been obtained, which contain snapshots of the operating conditions of LDPE tubular reactors including reactor pressure, temperature profiles, inlet and outlet cooling jacket temperatures, reactor conversion, and the entire set of flow rates, compositions, and temperatures of the axial feeds. The data sets also correspond to reactors with different configurations (number and arrangement of cooling and reaction zones, side feeds, CTAs, and initiator mixtures), which also produce different homo- and copolymer grades with different properties measured in terms of the macromolecular polymer properties and density. General ranges of typical number- and weight-average molecular weights and degrees of LCB for each grade have been provided as well.

The main objective of the parameter estimation procedure is to find the best set of on-line adjustable parameters and kinetic parameters that are best able to fit the reactor operating conditions for all data sets provided.

5.1. Estimation of On-Line Adjustable Parameters. As a first step in the estimation approach, we consider the estimation of the initiator efficiencies and heat transfer coefficients for every data set provided. These parameters are usually updated on-line to match the reactor temperature profile and the jackets inlet and outlet temperatures and to predict the reactor conversion and polymer properties obtained. Obviously, a better temperature profile match will be reflected directly in a more robust prediction of the reactor conversion and polymer properties.

For the *base case*, we consider a simplified estimation approach used currently as an industry standard. The strategy follows a sequential or feasible path approach as the one described in the previous section. In this strategy, a single efficiency is assumed for the entire initiator mixture in every reaction zone. Each of these efficiencies is assumed to be constant along its corresponding zone. The heat transfer coefficients (HTCs) are estimated for every cooling and reaction zone and are assumed to be constant along each zone as well. Furthermore, the parameters are estimated sequentially along the reactor, that is, solving for one zone at a time. This approach is followed in most studies because the resulting estimation problems are relatively small and simple to solve.[17]

On the other hand, in this work we propose to estimate the efficiency, $\eta_{i,j}$ for every initiator in the mixture fed to every reaction zone. The efficiencies are assumed to be constant along every zone. In addition, we estimate the HTCs for every zone, which are assumed to be constant along their corresponding zones as well. This approach leads to difficult problems with many parameters. The set of parameters defining each zone can

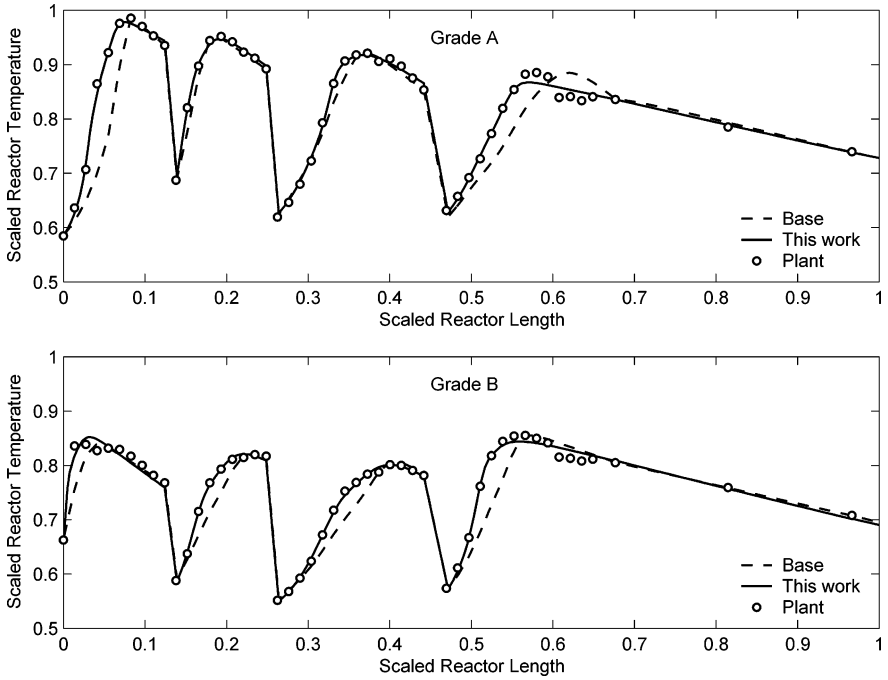

Figure 2. Plant and predicted temperature profiles using the base and the proposed estimation strategies for two different grades.

Table 2. Optimal Objective Function (OF) Values for the Estimation Approaches Analyzed, Grades A and B Cases

grade	OF−base	OF−this work	improvement
A	13 262.28	6628.43	50.02
B	17 474.44	4458.40	74.48

be estimated sequentially as well. However, due to the *downstream interaction* of these parameters, it is recognized that the entire set of on-line parameters must be estimated all-at-once for the *entire* reactor in a single, large estimation problem.

For the first case, we consider the match of two temperature profiles in different ranges describing the production of two different polymer grades (A and B) in the same reactor. Grade A is a copolymer with high comonomer content and grade B is a homopolymer, both of them being of high molecular weight. The reactor under study contains 13 zones, but only the first few reaction zones are presented. In Figure 2, the plant and predicted profiles using the base and the proposed all-at-once estimation approaches are presented. It is evident that the consideration of the individual efficiencies in the all-at-once approach has a strong impact on the initial shaping of the profiles in the reaction zones. This is attributed to the fact that the individual contributions of the different initiators in the mixture are now considered at different temperature levels along each reaction zone. The improvements in the match are more notable from the results presented in Table 2. For both approaches, we present the optimal values of the objective function, i.e., the sum of squares of deviations between the plant and predicted temperatures along the reactor and jackets. It is clear that the proposed approach is superior in both cases.

A direct consequence of having a better temperature profile match is the more accurate and consistent prediction of the overall reactor conversion, which plays a central role in the prediction of the polymer properties. In Figure 3, we present the conversion predicted by the model using the simplified estimation strategy and the one proposed in this work against the plant conversion. Twenty different grades, considering wide ranges of operating conditions and polymer properties are presented in the graph. The proposed approach gives a more consistent and accurate prediction. For the twenty grades, the

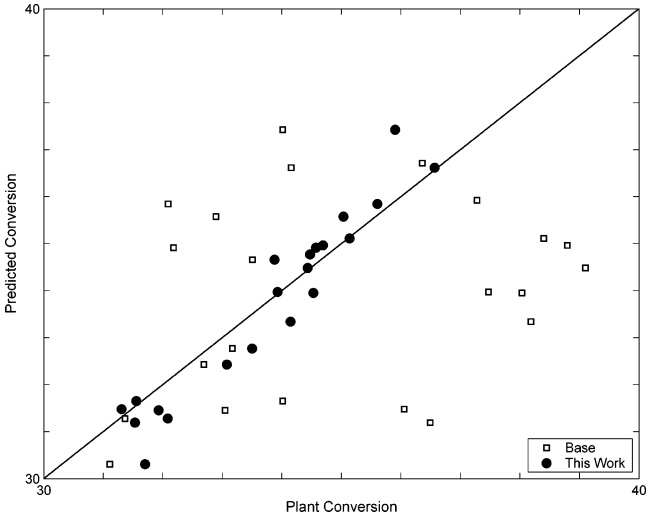

Figure 3. Plant and predicted conversions for the estimation approaches analyzed, results for 20 different grades.

average conversion deviation was reduced from 12.1% using the base case estimation strategy to 2.5% with the proposed all-at-once approach.

Both temperature profiles presented in Figure 2 were obtained by solving single-set parameter estimation problems. A total of 16 finite elements for the reaction zones, 2 finite elements for the cooling zones, and 3 collocation points were used for the discretization of the reactor model. To test different initialization strategies for the resulting NLPs, additional experiments were carried out using the solutions obtained from the sequential or feasible path strategy. For the zone-by-zone estimation of the on-line parameters, this strategy required only 20−30 CPUs for the on-line adjustable parameters. Around 80−90% of the solution time was spent for the integration of the reactor model equations for every zone. However, this approach was found to be expensive for the solution of the overall estimation problem since, in this case, the entire reactor model needs to be integrated at every iteration, taking around 4.5 CPUs per iteration. Following this reasoning, the approach was expected to become

Table 3. Computational Results for Single-Set NLP Problems, On-Line Parameter Estimation Case Studies[a]

grade	constraints	parameters	LB	UB	iterations	CPUs	NZJ	NZH
A	11 955	32	374	361	11	17.03	166 425	87 954
B	11 283	32	374	361	8	10.06	138 666	76 890

[a] LB = number of lower bounds; UB = number of upper bounds; NZJ = number of nonzeros in Jacobian; NZH = number of nonzeros in Hessian.

Table 4. Confidence Intervals for On-Line Adjustable Parameters, Grade A Case

zone	initiator 1	initiator 2	initiator 3	HTC
1	0.2294 ± 0.0166	0.0736 ± 0.0067	0.1055 ± 0.0053	0.3120 ± 0.0138
2	0.2365 ± 0.0258	0.0939 ± 0.0011	0.0903 ± 0.0082	0.2325 ± 0.0182
3	0.2051 ± 0.0202	0.2028 ± 0.0156	0.1521 ± 0.0143	0.3277 ± 0.0153
4	0.3817 ± 0.0327	0.1970 ± 0.0157	0.1322 ± 0.0137	0.2887 ± 0.0148

extremely expensive for the solution of multiset and EVM problems and, therefore, was not considered further in this study.

On the other hand, significant reductions on the overall CPU time were obtained using the proposed simultaneous approach. The computational results associated with the solution of the corresponding large-scale NLPs are presented in Table 3. The optimization problems were solved on a 3.0 GHz, 1 Gb RAM, Pentium IV PC. Since a good starting point is provided in all cases to the algorithm, a small initial barrier parameter μ of 1×10^{-6} was set for all calculations. In all cases, the model was initialized with the solution of the zone-by-zone simplified estimation strategy. In both cases, the Hessian matrix was found to be positive definite at the solution with large eigenvalues ranging from 10^2 to 10^{10}. Since inertia correction was not necessary at the solution, we can conclude that the parameters are unique. The NLPs are quite large with around 10 000 constraints and 32 degrees of freedom (corresponding to the entire set of on-line adjustable parameters). Nevertheless, the solution approach is fast and reliable, taking around 1.5 CPUs per iteration, compared to the 4.5 CPUs per iteration found by following the feasible path approach. The fast and reliable solutions obtained with the proposed method motivates the solution of more complex parameter estimation problems which are crucial for further development and on-line update of the first-principles reactor model.

In Table 4, we present the values of the on-line adjustable parameters for the Grade A case and their corresponding 95% confidence intervals. The confidence intervals were obtained following standard methods that approximate the covariance matrix using the reduced Hessian at the solution of the optimization problems.[28] It is worth noticing that the initiator efficiencies are adjustable factors that compensate for any plant−model mismatch and, as a consequence, their actual values will depend on the values of the rest of the kinetic parameters in the model, for example, the initiator decomposition rate constants. On the other hand, the values of the heat transfer coefficients are well in the range of typical observed values in industrial reactors.[9] Similar results were obtained for the Grade B case; hence, the estimation procedure is consistent.

5.2. Estimation of Kinetic Parameters. The estimation approach presented in the previous section gives a robust and accurate match of the reactor temperature profile. Once the model is able to match this profile, we can predict the reactor conversion, the polymer macromolecular properties, and the final end-use properties such as the polymer density. Here, we also need to estimate parameters for the kinetic constants that apply to *multiple* data sets over different ranges of operating conditions. The kinetic rate constants presented in Table 1 have the following form

$$k_i = k_i^0 \exp\left[-\frac{\Delta E_{ai} + P\Delta E_{vi}}{RT}\right] \qquad (48)$$

where subindex i belongs to the entire set of elementary reactions in the kinetic mechanism. Symbol k_i^0 denotes the preexponential factor, ΔE_{ai}, the activation energy, ΔE_{vi}, the activation volume, and P, the reactor pressure.

Since the number of parameters is so large, it has been common in previous studies to make certain assumptions and decompose the estimation procedure into subproblems with fixed subsets of parameters.[1,5,8] In these approaches, a first step is to estimate the propagation and termination kinetic rate constants to match the reactor overall conversion. The second step consists of estimating other kinetic parameters to match macromolecular properties such as number- and weight-average molecular weights, LCB, and polymer density. This iterative approach is repeated until the best set of parameters is obtained. This approach is obviously nonsystematic and time-consuming.

The ideal approach to solving these complex parameter estimation problems is to include a large number of informative data sets describing the operation of different reactors over wide ranges of operating conditions, for homo- and copolymers, using different CTAs, initiators, and producing grades with different molecular and structural properties, and to estimate the whole set of kinetic parameters in a single and very large parameter estimation problem. Furthermore, since on-line adjustable parameters depend on the kinetic parameters, they need to be included in the estimation problem, giving rise to an even larger and more complicated problem.

Following the all-at-once approach in this work, it is possible to solve challenging multiset parameter estimation problems. This enables more efficient and systematic strategies to be developed for the estimation of the kinetic parameters using industrial data.

5.2.1. Homopolymerization Case Study. As a first step, we consider the estimation of the kinetic parameters for homopolymerization reactions. The homopolymer grades are produced on the same reactor operating over different ranges of temperature, pressure, and concentration of a single CTA. Common values of the macromolecular properties for the different grades are used in this problem. For all the problems solved, the entire set of on-line and kinetic parameters is estimated to match the reactor and jacket temperatures, overall reactor conversion, number- and weight-average molecular weights, polymer density, and degree of long-chain branching (LCB).

The motivation behind the use of multiple data sets for the estimation of the kinetic parameters becomes clear from Figure 4. Here, two different 95% ellipsoidal confidence regions are presented for the propagation rate constant (k_{p11}) preexponential factor and activation energy. The ellipsoids were obtained from the solution of estimation problems with one and three data sets. It is clear that there is a large uncertainty associated with point estimation of the preexponential factor that solves the single-set problem. However, a single set is informative enough to have a tight confidence interval for the activation energy since

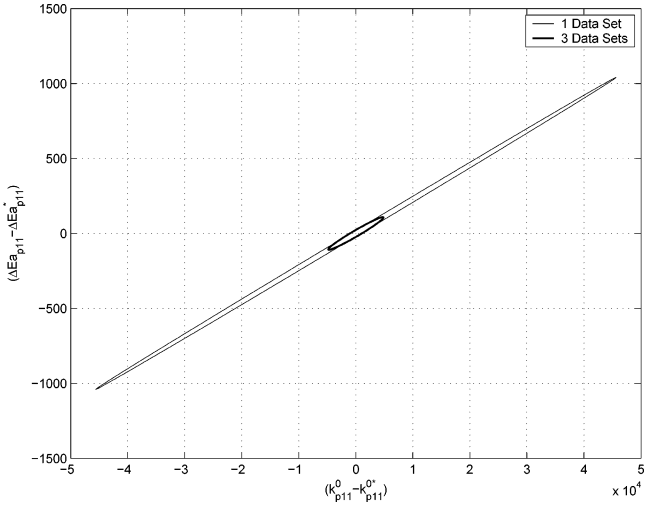

Figure 4. Confidence regions for the parameters of the propagation rate constant k_{p11}, results for problems with 1 and 3 data sets.

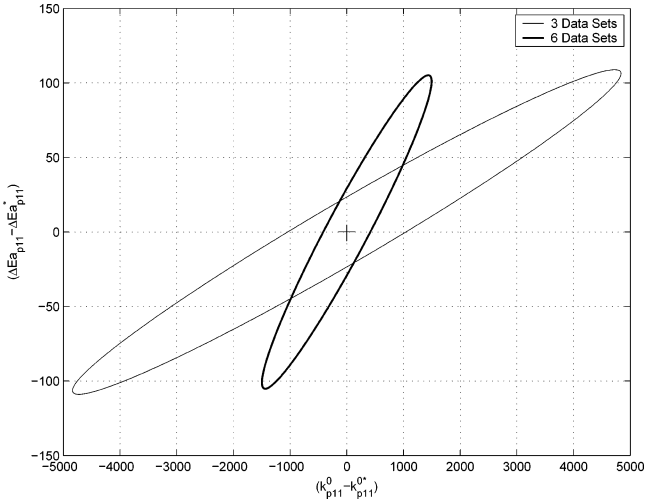

Figure 5. Confidence regions for the parameters of the propagation rate constant k_{p11}, results for problems with 3 and 6 data sets.

every set describes the reactor behavior over a wide range of temperature. In Figure 5, the confidence regions from the solution of problems having 3 and 6 data sets are presented. The ellipsoid obtained from the 6 sets problem is even smaller, and the parameter estimates seem to have tight enough confidence intervals.

Multiset estimation problems were solved using the standard least-squares and EVM formulations. The reformulated model described in the previous section is used in these problems. The computational results are presented in Table 5. The resulting NLP size increases linearly with the number of data sets. For the EVM formulation, we have many more degrees of freedom, which also increase linearly. Thus, for standard least-squares, we estimate 32 on-line adjustable parameters for each data set along with 28 kinetic parameters; the heat of polymerization is estimated as well. For the EVM formulation, the degrees of freedom for every set are increased by 52 input variables. In all cases, the estimation problems are initialized from a good starting point using the optimal values of the on-line adjustable parameters obtained in the previous section. Accordingly, an initial barrier parameter μ was set to a small value of 1×10^{-6} for all the calculations. Other than this, the default algorithmic parameters of the optimization algorithm were used. It is interesting to analyze the performance of the algorithm in the solution of these large-scale NLPs. The number of iterations remains consistent among the different problems and in a range typical of interior-point methods. The sparsity pattern of the linear system (43) is almost unaltered between formulations. This might explain the similar computational times required by the algorithm despite the increase in the degrees of freedom. The availability of exact first and second order derivative information is also crucial. The largest estimation problem was solved in less than 20 min on a 3.0 GHz, 1 Gb RAM, Pentium IV PC. Problems with more data sets were not solved due to limitations in memory requirements associated with the storage of the large and relatively sparse iteration matrix. Furthermore, it was decided to solve the problems only with standard computational resources. A fast and efficient approach to the solution of problems with dozens of data sets aiming to overcome this problem is described in the last section of the paper.

For the parameter estimation, we assume the initiation and propagation rate constants to be equal. We also determined that the combined estimation of the initiator efficiencies and the initiator decomposition rate constants leads to nonunique solutions. Therefore, the decomposition rate parameters were fixed and rate constants for termination by combination and disproportionation were assumed to be equal. With these assumptions, the obtained parameter values lie well between reported ranges[4] but the activation volumes for the propagation, chain transfer to monomer, and backbiting reactions have opposite signs to those usually reported. Also, the β-scission reaction rate parameters are not observable from the data. These can be estimated only if information such as vinylenes and vinylidenes content is included in the problem. Unfortunately, this information was not available.

On the other hand, with the previous base set of parameters, the model could not predict the effect of large variations of pressure on the weight-average molecular weight. This effect might be due to the polymerization mechanism itself or to physical phenomena (for instance, a decreased polymer solubility in the gas phase) not considered by the model. With the new set of estimated parameters, the model was able to predict this pressure effect, and the estimated activation volumes are clearly compensating for this effect.

Finally, the model predictions were notably improved using the new set of parameters. This is clearly depicted in Figure 6 where plant and model predictions for the overall reactor conversion, number- and weight-average molecular weights and degree of LCB are presented. Here, we consider a total of six estimation and eight validation cases including different reactor configurations and wide ranges of operating conditions. These grades span a range of 30−37% on the overall reactor conversion, 14 500−19 500 g/gmol on the number-average molecular weight, 150 000−450 000 g/gmol on the weight-average molecular weight, and 2.4−2.8 on the number of LCBs per 1000 carbon atoms. Average values of the deviations between the model predictions and the plant measurements for different polymer properties are presented in Table 6. Here, we present model deviations using the base industrial set of kinetic parameters provided and the new parameters obtained in this work. The predictions using the new set clearly outperform those obtained using the base set in all cases.

5.2.2. Copolymerization Case Study. Some of the polymer grades consist of LDPE copolymers of high molecular weight and low comonomer content. Using the optimal set of parameters for the homopolymerization reactions, the next step is to estimate the kinetic parameters for the rate constants of the copolymerization reactions. The best approach to solving this

Table 5. Computational Results for Multiple-Set NLP Problems, Homopolymerization Case Study[a]

data sets	constraints	DOF	LB	UB	iterations	CPUs	NZJ	NZH
3	33 900	121	1246	1207	68	451.51	520 275	552 738
3 (EVM)	33 952	277	1366	1327	57	345.82	520 636	553 080
6	68 421	217	2467	2389	58	900.21	1 058 412	1 119 258
6 (EVM)	68 627	529	2653	2575	71	1010.74	1 059 512	1 119 780

[a] LB = number of lower bounds; UB = number of upper bounds; NZJ = number of nonzeros in Jacobian; NZH = number of nonzeros in Hessian; DOF = degrees of freedom.

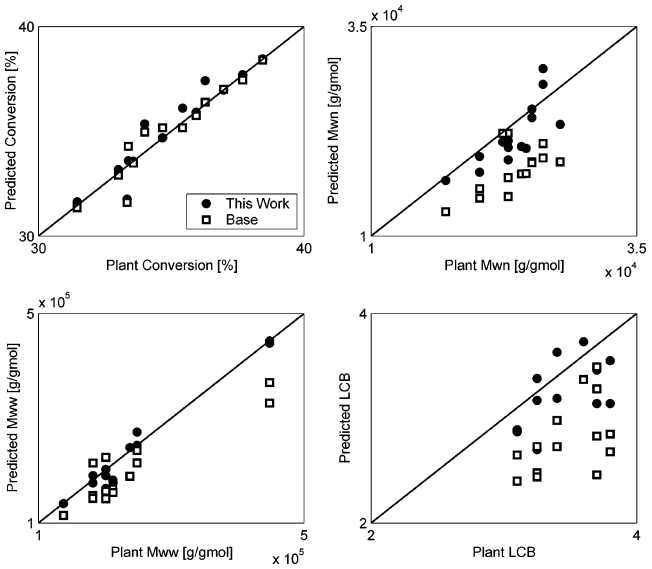

Figure 6. Homopolymer grade macromolecular properties, plant and model predictions.

problem would be to consider a large multiset estimation problem including both homo- and copolymer grades to estimate the whole set of kinetic parameters. However, the optimization problems resulting from the copolymerization cases are significantly more expensive to solve.

The estimation of the copolymerization kinetic parameters was performed with a three data set estimation problem. Only the parameters corresponding to the copolymerization reactions were estimated; the homopolymerization parameters were fixed at their optimal values. The copolymer grades data sets are not highly informative since these grades are produced under limited ranges of operating conditions and the resulting polymer properties are quite similar. Therefore, even if many data sets could be handled in a single problem to estimate the whole set of kinetic parameters, there would not be a significant reduction in the parameter confidence intervals. Table 7 summarizes the computational results for the solution of the standard least-squares and EVM problem. A total of 32 on-line adjustable parameters was estimated for every data set along with 22 kinetic parameters. Both problems were solved in a similar number of iterations. Interestingly, the algorithm required less CPU time for the EVM problem than the standard problem. Nevertheless, a solution of these problems is more expensive than for homopolymerization due to it having more constraints and a denser structure for the Jacobian matrix.

For copolymerization, the resulting confidence intervals are not as tight as for the homopolymerization case. This can be attributed to the small number of sets used in the estimation problem or to a lack of informative data. The three grades used in the estimation are obtained at a similar reactor pressure, so there is a large uncertainty associated with the activation volumes for the different rate constants. The chain transfer to monomer and comonomer rate constants k_{fm21} and k_{fm22} cannot be estimated reliably using the data provided. Furthermore, the

Table 6. Average Deviations between Plant and Model Predictions for Reactor Conversion and Grade Macromolecular Properties[a]

parameter set	conversion (%)	MW_n (%)	MW_w (%)	LCB (%)	density (%)
base	1.49	23.24	18.58	19.20	0.0965
new	0.12	6.20	3.31	6.27	0.0875

[a] Results for 14 different grades, homopolymerization case study.

kinetic parameters for the backbiting rate constant k_{b2} and the heat of polymerization, ΔH_{r2}, do not seem to have a strong effect on the model. We also note that the model is limited in the prediction of the degree of LCB for the copolymer grades. This is due to the fact that our base kinetic mechanism assumes that the addition of copolymer does not have a strong effect on the chain transfer to polymer reactions. Unfortunately, the assumption cannot be corroborated since the related kinetic parameters cannot be estimated reliably using the data provided, as discussed previously.

Nevertheless, as in the homopolymerization case, the model predictions were notably improved for the copolymerization case as well. This can be noted from Figure 7. In this case, three estimation and three validation sets were considered. The grades span a range of 33−37% on the overall reactor conversion, 22 000−29 000 on the number-average molecular weight, 200 000−350 000 on the weight-average molecular weight, 2.9−3.6 on the number of LCBs per 1000 carbon atoms, and 2−6% on the copolymer composition. Improved predictions were obtained over the full range of the polymer properties using the new set of kinetic parameters. In Table 8, the average deviations of the polymer properties and the overall reactor conversion are presented. Again, the model predictions with the new set of parameters outperform those obtained using the base set provided from industry.

6. Conclusions and Future Work

We propose a simultaneous, or all-at-once, approach for the solution of large-scale DAE-constrained parameter estimation problems. The estimation problems arise from model development and on-line estimation tasks of first-principles models for LDPE reactors. The solution strategy allows the robust and efficient solution of large multiset parameter estimation problems with up to 200 parameters. Challenging parameter estimation strategies such as the errors-in-variables-measured (EVM) formulation can be handled in a straightforward manner under this approach. Here, multiset EVM estimation problems with up to 70 000 constraints and over 500 degrees of freedom can be solved quickly and efficiently with standard computational resources. The use of robust and efficient large-scale nonlinear programming algorithms is fundamental for the solution of the associated large-scale NLP problems. Following the systematic estimation strategy, reliable parameter estimates could be estimated directly from industrial plant data using the rigorous reactor model. Also, notable improvements in the model predictions were found using the estimated parameters.

There is a natural motivation to solve estimation problems with as much informative data as possible, in order to find more

Table 7. Computational Results for Multiple-Set NLP Problems, Copolymerization Case Study[a]

data sets	constraints	DOF	LB	UB	iterations	CPUs	NZJ	NZH
3	35 868	118	1249	1210	89	1008.75	636 891	657 880
3 (EVM)	35 973	289	1351	1312	84	751.14	637 467	658 150

[a] LB = number of lower bounds; UB = number of upper bounds; NZJ = number of nonzeros in Jacobian; NZH = number of nonzeros in Hessian; DOF = degrees of freedom.

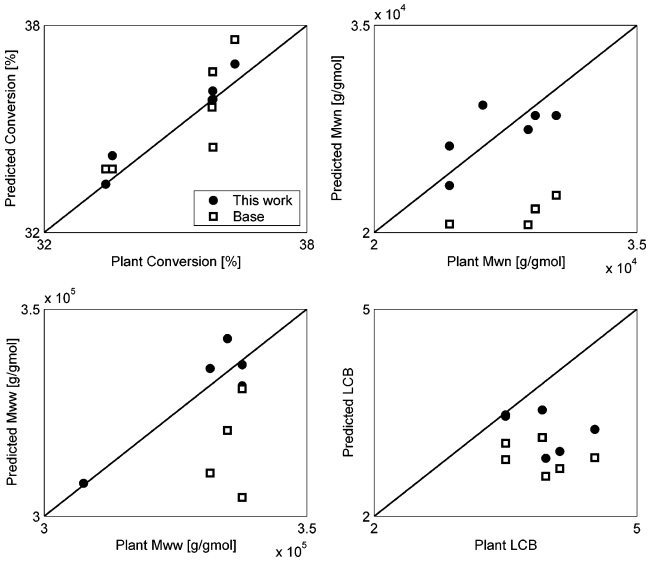

Figure 7. Copolymer grade macromolecular properties, plant and model predictions.

Table 8. Average Deviations between Plant and Model Predictions for Reactor Conversion and Grade Macromolecular Properties[a]

parameter set	conversion (%)	MW_n (%)	MW_w (%)	LCB (%)	density (%)
base	2.03	24.48	6.13	26.40	0.262
new	0.37	8.29	1.83	16.64	0.095

[a] Results for 6 different grades, copolymerization case study.

reliable parameter estimates. However, beyond the problems addressed here, there is a limitation in both memory and CPU time requirements for the solution of highly complex multiset estimation problems, using current standard computational resources. These limitations can be overcome through specialized decomposition strategies[50] that are able to exploit the structure of the parameter estimation problems (35)−(36). For instance, recalling the EVM problem formulation, two different sets of variables can be identified. The first set affects *only* a particular data set k ($p_{k,j}$ and $u_{k,j}$). These variables include the initiator efficiencies, the heat transfer coefficients, and the input variables for the given data set. The second set of variables, i.e., the kinetic parameters, appear in the constraints of all the data sets (Π). This means that the only complicating variables between the entire set of constraints in the optimization problem is the small subset of variables Π. Therefore, the resulting NLP problem obtained from the discretization of the parameter estimation problem can be viewed as a multiscenario optimization problem.[49] These problems give rise to a very particular and well-defined arrowhead or block-bordered diagonal structure of the linear system (43). A straightforward decomposition strategy can be applied to this system, leading to the serial or parallel solution of smaller linear systems corresponding to each data set and, thus, overcoming memory and CPU time limitations.

Finally, a recent object-oriented re-implementation of IPOPT permits a flexible environment for the implementation of tailored linear algebra strategies, thus allowing the solution of challenging large-scale optimization problems with exploitable structures such as the particular ones arising from parameter estimation.[51] The application of this approach will be the subject of a future study.

Acknowledgment

We would like to thank Andreas Wächter and Carl Laird for the insightful discussions pertaining to efficient use of IPOPT for the solution of large-scale optimization problems.

Notation

A = reactor cross-sectional area, m^2
C_j = molar concentration of jth component, kgmol/m^3
C_p = reacting mixture heat capacity, kJ/kg·K
C_{pc} = cooling agent heat capacity, kJ/kg·K
D_i = reactor internal diameter, m
$D_{r,s}$ = concentration of dead polymer chains with r monomer units and s comonomer units, kmol/m^3
F_j = molar flow rate of the jth component, kgmol/s
F_c = cooling agent flow rate, kg/s
f_r = Fanning friction factor
HTC = heat transfer coefficient, kW/m^2·K
k_{bi} = intramolecular (backbiting) chain transfer of live polymer chains of type i, 1/s
k_{di} = decomposition rate constant of the ith initiator, 1/s
k_{Ii} = initiation rate constant for the ith monomer, m^3/gmol·s
k_{fmij} = rate constant for the transfer of live polymer chains of type i to the j monomer, m^3/gmol·s
k_{fpij} = rate constant for the transfer of dead polymer chains of type i to the j monomer, m^3/gmol·s
k_{pij} = propagation rate constant for the live polymer chains ending in the ith monomer unit with the jth monomer, m^3/gmol·s
k_{sij} = rate constant for transfer of live polymer chains of type i to chain-transfer agent j, m^3/gmol·s
k_{spij} = rate constant for incorporation of CTA j to live polymer chains of type i, m^3/gmol·s
k_{tcij} = termination by combination rate constant, m^3/gmol·s
k_{tdij} = termination by disproportionation rate constant, m^3/gmol·s
$k_{\beta i}$ = β-scission rate constant for secondary radicals, 1/s
$k'_{\beta i}$ = β-scission rate constant for tertiary radicals, 1/s
LCB = number of long-chain branches per 1000 carbon atoms
MW_n = number-average molecular weight, kg/kgmol
MW_w = weight-average molecular weight, kg/kgmol
MW_0 = molecular weight of a building unit, kg/kgmol
N_I = number of initiators
N_S = number of chain-transfer agent(s)
P = reactor pressure, atm
R_i = total concentration of live polymer chains ending in a radical of type i, kgmol/m^3
SCB = number of short-chain branches per 1000 carbon atoms
T = reactor temperature, K
T_c = cooling agent temperature, K
v = fluid velocity, m/s

Greek Letters

$-\Delta H_{ri}$ = heat of reaction for the ith monomer, kJ/kgmol
η_i = efficiency of the ith initiator in the mixture
λ_n^i = nth order single moment of the live polymer chains of type i, kgmol/m^3
μ_n = nth order single moment of the dead polymer chains, kgmol/m^3
ρ_m = reacting mixture density, kg/m^3
ρ_{pol} = polymer density, g/cm^3

Subscripts

Ii = ith initiator
Si = ith chain-transfer agent
mi = ith monomer
R = primary radicals

Literature Cited

(1) Kiparissides, C.; et al. Mathematical Modeling of Free-Radical Ethylene Copolymerization in High-Pressure Tubular Reactors. *Ind. Eng. Chem. Res.* **2005**, *44*, 2592−2605.

(2) Goto, S.; et al. Computer Model for Commercial High-Pressure Polyethylene Reactor Based on Elementary reaction Rates Obtained Experimentally. *J. Appl. Pol. Sci.* **1981**, *36*, 21−40.

(3) Zabisky, R. C. M.; Chan, W. M.; Gloor, P. E.; Hamielec, A. E. A Kinetic Model for Olefin Polymerization in High-Pressure Tubular Reactors. A Review and Update. *Polymer* **1992**, *33*, 2243−2262.

(4) Kiparissides, C.; Verros, G.; McGregor J. Mathematical Modeling, Optimization and Quality Control of High-Pressure Ehtylene Polymerization Reactors. *J. Macromol. Sci., Rev. Macromol. Chem. Phys.* **1993**, *C33*, 437−527.

(5) Brandolin, A.; Lacunza, P.; Ugrin, L.; Capiati, N. J. High-Pressure Polymerization of Ethylene and Improved Mathematical Model for Industrial Tubular Reactors. *Polym. React. Eng.* **1996**, *4*, 193−241.

(6) Kim, D. M.; Iedema, P. D. Molecular Weight Distribution in Low-Density Polyethylene Polymerization; Impact of Scission Mechanisms in the Case of a Tubular Reactor. *Chem. Eng. Sci.* **2004**, *59*, 2039−2052.

(7) Achilias, D. S.; Kiparissides, C. Towards the Development of a General Framework for Modeling Molecular Weight and Compositional Changes in Free Radical Copolymerization Reactions. *J. Macromol. Sci., Rev. Macromol. Chem. Phys.* **1992**, *C32*, 183.

(8) Bokis, C. P. Physical Properties, Reactor Modeling, and Polymerization Kinetics in the Low-Density Polyethylene Tubular Reactor Process. *Ind. Eng. Chem. Res.* **2002**, *41*, 1017−1030.

(9) Buchelli, A.; et al. Modeling Fouling Effects in LDPE Tubular Polymerization Reactors. 1. Fouling Thickness Determination. *Ind. Eng. Chem. Res.* **2005**, *44*, 1474−1479.

(10) Singstad, P. Modeling and Multivariable Control of High-Pressure Autoclave Reactors for Polymerization of Ethene. Ph.D. Thesis, NTNU, Norway, **2002**.

(11) Faber, R.; Li, P.; Wozny, G. Sequential Parameter Estimation for Large-Scale Systems with Multiple Data Sets. 1. Computational Framework. *Ind. Eng. Chem. Res.* **2003**, *42*, 5850−5860.

(12) Tjoa, I. B.; Biegler, L. T. Simultaneous Solution and Optimization Strategies for Parameter Estimation of Differential-Algebraic Equation Systems. *Ind. Eng. Chem. Res.* **1991**, *30*, 376−385.

(13) Sirohi, A.; Choi, K. Y. On-line Parameter Estimation in a Continuous polymerization process. *Ind. Eng. Chem. Res.* **1996**, *35*, 1332−1343.

(14) Bindlish, R.; Rawlings, J. B.; Young, R. E. Parameter estimation for Industrial Polymerization Processes. *AICHE J.* **2003**, *49*, 2071−2078.

(15) Arora, N.; Biegler, L. T. Parameter Estimation for a Polymerization Reactor Model with a Composite-Step Trust-Region NLP Algorithm. *Ind. Eng. Chem. Res.* **2004**, *43*, 3616−3631.

(16) Wächter, A.; Biegler, L. T. On The Implementation of an Interior-Point Filter Line-Search Algorithm for Large-Scale Nonlinear Programming. *Math. Programming* **2006**, *106*, 25−57.

(17) Kiparissides, C.; Verros, G.; Pertsinidis, A.; Goosens, I. On-Line Parameter Estimation in a High-Pressure Low-Density Polyethylene Tubular Reactor. *AICHE J.* **1996**, *42*, 440.

(18) Ray, W. H. On the Mathematical Modeling of Polymerization Reactors. *J. Macromol. Sci. ,Rev. Macromol. Chem. Phys.* **1972**, *C8*, 1.

(19) Lee, B. I.; Kesler, M. G. A Generalized Thermodynamic Correlation Based on a Three-Parameter Corresponding States. *AICHE J.* **1975**, *21*, 510−527.

(20) Verros, G.; Papadakis, M.; Kiparissides, C. Mathematical Modeling of High-Pressure Tubular LDPE Copolymerization Reactors. *Polym. React. Eng.* **1993**, *1*, 427−460.

(21) Yoon, W. J.; Kim, Y. S.; Kim, I. S.; Choi, K. Y. Recent Advances in Polymer Reaction Engineering: Modeling and Control of Polymer Properties. *Korean J. Chem. Eng.* **2004**, *21*, 147−167.

(22) Buchelli, A.; et al. Modeling fouling effects in LDPE tubular polymerization reactors. 2. Heat transfer, computational fluid dynamics, and phase equilibria. *Ind. Eng. Chem. Res.* **2005**, *44*, 1480−1492.

(23) Lacunza, M.; Ugrin, P. E.; Brandolin, A.; Capiati, N. J. Heat Transfer Coefficient in a High-Pressure Tubular Reactor for Ethylene Polymerization. *Polym. Eng. Sci.* **1998**, *38*, 992−1013.

(24) Luft, G.; et al. Effectiveness of Organic Peroxide Initiators in the High-Pressure Polymerization of Ethylene. *J. Macromol. Sci., Chem.* **1977**, *A11*, 1089−1112.

(25) Seidl, H.; Luft, G. Peroxides as Initiators for High-Pressure Polymerization. *J. Macromol. Sci., Chem.* **1981**, *A15*, 1−33.

(26) Moran, P. A. P. Estimating Structural and Functional Relationships. *J. Multivar. Anal.* **1971**, *1*, 192−199.

(27) Kendall, M. G.; Stuart, A. *The Advanced Theory of Statistics*; Griffin, London, 1973.

(28) Bard, Y. *Nonlinear Parameter Estimation*; Academic Press: Cambridge, MA, **1974**.

(29) Kim, I. W.; Liebman, M. J.; Edgar, T. F. A Sequential Error-in-Variables Method for Nonlinear Dynamic Systems. *Comput. Chem. Eng.* **1991**, *15*, 663−670.

(30) Caracotsios, M.; Stewart, W. E. Sensitivity Analysis of Initial Value Problems with Mixed ODEs and Algebraic Equations. *Comput. Chem. Eng.* **1985**, *9*, 359−366.

(31) Binder, T. L.; Blank, H. G.; Bock, R.; Burlisch, W.; Dahmen, M.; Diehl, T.; Kronseder, W.; Marquardt, J. P.; Schlder, O. v. Stryk, Introduction to Model Based Optimization of Chemical Processes on Moving Horizons. In *Online Optimization of Large Scale Systems*; Grtschel, M., Krumke, S. O., Rambau, J., Eds.; Springer-Verlag: Berlin, Heidelberg, 2001; pp 295−339.

(32) Vassiliadis, V. S.; Sargent, R. W. H.; Pantelides, C. C. Solution of a class of multistage dynamic optimization problems. 1. Problems without path constraints. *Ind. Eng. Chem. Res.* **1994**, *33*, 2111−2122.

(33) Teo, K.; Goh, G.; Wong, K. A Unified Computational Approach to Optimal Control Problems. *Pitman Monographs and Surveys in Pure and Applied Mathematics*; Wiley: New York, 1991.

(34) Biegler, L. T.; Grossmann, I. E. Retrospective on Optimization. *Comput. Chem. Eng.* **2004**, *28*, 1169−1192.

(35) Biegler, L. T.; Cervantes, A. M.; Wächter, A. Advances in Simultaneous Strategies for Dynamic Process Optimization. *Chem. Eng. Sci.* **2002**, *57*, 575−593.

(36) Byrd, R. H.; Gilbert, J. Ch.; Nocedal, J. A Trust-Region Method Based on Interior-Point Techniques for Nonlinear Programming. *Math. Programming* **2000**, *89*, 149−185.

(37) Benson, H. Y.; Shanno, D. F.; Vanderbei, R. J. Interior-Point Methods for Nonconvex Nonlinear Programming: Filter Methods and Merit Functions. *Comput. Opt. Appl.* **2002**, *23*, 257−272.

(38) Fourer, R.; Gay, D. M.; Kernighan, B. W. *AMPL: A Modeling Language for Mathematical Programming*; Duxbury Press: Belomont, CA, 1992.

(39) Brooke, A.; Kendrick, D.; Meeraus, A.; Raman, R. *GAMS-A users guide*; 1998.

(40) Biros, G.; Ghattas, O. Parallel Lagrange-Newton-Krylov-Schur Methods for PDE Constrained Optimization. Part I: The Krylov-Schur Solver. *SIAM J. Sci. Comput.* **2003**, *27*, 687.

(41) Betts, J.; Huffman, W. P. Large-Scale Parameter Estimation Using Sparse Nonlinear Programming Methods. *SIAM J. Optim.* **2003**, *14*, 223−244.

(42) Kawajiri, Y.; Biegler, L. T., Optimization strategies for simulated moving bed and PowerFeed processes. *AIChE J.* **2006**, *49*, 1343−1350.

(43) Bader, G.; Ascher, U. A New Basis Implementation ofr Mixed Order Boundary Value ODE solvers. *SIAM J. Sci. Comput.* **1987**, *8*, 483−500.

(44) Fiacco, A. V.; McCormick, G. P. *Nonlinear Programming. Sequential Unconstrained Minimization Techniques*; SIAM: Philadelphia, PA, 1990.

(45) Duff, I. S.; Reid, J. K. *MA27: A set of Fortran Subroutines for Solving Sparse Symmetric Sets of Linear Equations*; technical report, Computer Science and Systems Division, AERE Harwell: Oxford, England, 1982.

(46) Vanderbei, R. J.; Shanno, D. F. An Interior-Point Algorithm for Nonconvex Nonlinear Programming. *Comput. Opt. Appl.* **1999**, *13*, 231−252.

(47) Poku, M. Y. B.; Biegler, L. T. Nonlinear Optimization with Many Degrees of Freedom in Process Engineering. *Ind. Eng. Chem. Res.* **2004**, *43*, 6803.

(48) Wächter, W. An Interior Point Algorithm for Large-Scale Nonlinear Optimization with Applications in Process Engineering. Ph.D. Thesis, Carnegie Mellon University, Pittsburgh, PA 2002.

(49) Biegler, L. T.; Grossmann, I. E.; Westerberg, A. W. *Systematic Methods of Chemical Process Design*; Prentice Hall: New Jersey, 1997.

(50) Biegler, L. T.; Tjoa, I. N. A Parallel Implementation for Parameter Estimation with implicit models. *Anns. Oper. Res.* **1993**, *42*, 1−23.

(51) Laird, C.; Biegler, L. T. A Block-Bordered Interior Point Approach for the Solution of Multiperiod Nonlinear Programs. Presented at the AIChE Annual Meeting, Cincinnati, OH, 2005.

Received for review March 20, 2006
Revised manuscript received August 28, 2006
Accepted August 30, 2006

IE060338N